On the Mechanism of the Plasmonic Field Enhancement of the Solar-to-Electric Energy Conversion by the Other Photosynthetic System in Nature (Bacteriorhodopsin): Kinetic and Spectroscopic Study

Li-Kang Chu,† Chun-Wan Yen,† and Mostafa A. El-Sayed*

Laser Dynamics Laboratory, School of Chemistry and Biochemistry, Georgia Institute of Technology, Atlanta Georgia 30332

Received: June 14, 2010; Revised Manuscript Received: July 22, 2010

We have recently reported Ag nanoparticles (AgNPs) plasmonic field enhancement of the Bacteriorhodopsin (bR) photocurrent observed during its proton pump photocycle in solution. We proposed a mechanism based on the plasmonic field enhancement of the blue light effect which bypasses the slow part of the photocycle and increases the rate of proton production and thus the observed photocurrent. In this present work, we studied the AgNPs plasmonic field effect on the spectroscopy and kinetics of the bR proton pumping photocycle. We examined the blue light effect on both the recovery rate of bR and the decay rate of the M intermediate by using 532-nm short-pulsed laser excitation of bR in the presence of AgNPs and continuous-wave blue light exposure. Our observation showed that the recovery of bR and the decay of the M intermediate are both greatly accelerated in the presence of both AgNPs and blue light simultaneously. This gives support for the proposed mechanism of the enhanced proton current in the presence of AgNPs with a plasmon band in the blue region. It was found experimentally that the 40 nm-AgNPs enhancement of the blue light effect on the decay rate is around 400× larger than that of 8 nm-AgNPs. This is found to be in agreement with the known dependence of the plasmonic field on size and the overlap of the plasmonic extinction band with the absorption band of the M intermediates.

1. Introduction

Bacteriorhodopsin (bR) is the other photosynthetic system in nature and is the transmembrane protein found in *Halobacterium salinarium*. It has been widely investigated due to its unique structural, optical, biochemical, and biophysical properties and is the best studied proton pump system in biology.[1–17] The purple membrane (PM) is composed mainly of protein (75% by wt.), with the remaining 25% being composed of lipids.[1] The lattice parameters of crystallized PM have been investigated extensively and are found to be composed of seven helices and one interior retinal chromophore per bR in the two-dimensional hexagonal structure.[2–6]

The light-adapted bR exhibits an intense characteristic retinal absorption band centered at 568 nm with a corresponding extinction constant of $\epsilon_{568} = 62\ 700\ M^{-1}\ cm^{-1}$.[7] Upon photoexcitation of bR, the corresponding transition from a ^1B_u-like ← S_0 state of the retinal chromophore gives rise to the isomerization from its all-trans conformation to the 13-cis conformation.[8] This is followed by the thermal formation of a series of spectrally distinguishable intermediates given by (eq 1).[9]

$$\begin{aligned} bR_{568} \xrightarrow{h\nu} I_{460} \xrightarrow{0.5ps} J_{625} \xrightarrow{3ps} K_{590} \xrightarrow{\sim 2\mu s} L_{550} \xrightarrow{50\mu s} \\ M_{412}(M_1 \rightarrow M_2) \xrightarrow{1ms} N_{560} \xrightarrow{2ms} O_{640} \xrightarrow{8ms} bR_{568} \end{aligned} \quad (1)$$

Following retinal isomerization, the proton translocation from the protonated Schiff base to Asp85 gives rise to the generation of the early M state (labeled M_1).[10–12] The structures of the initial state and the early intermediates (K, L, and M_1) are proposed to have one protein conformation in which the Schiff base has extracellular accessibility.[13] A consequential proton release to the extracellular side of the protein, via Glu194, Glu204, and the structure chain of water molecules, occurs during the conversion of M_1 to M_2 (labeled late M).[14,15] M_1 and M_2 are spectrally characterized by absorption at 410 nm with a corresponding extinction constant of 48 800 $M^{-1}\ cm^{-1}$.[16]

A sequential reprotonation of the Schiff base from Asp96 results in the generation of the N intermediate followed by the generation of the O intermediate involving the 13-cis to all-trans isomerization of the retinal.[17] The transition of O → bR occurs via the relaxation of the protein structure to give bR_{568} and completes the photocycle (eq 1).

When the photocycle is exposed to blue light, the long-lived blue light absorbing M_{412} intermediate is converted to bR_{568} in hundreds of nanoseconds (eq 2). This shortcut greatly reduces the conventional photocycle period which takes 15 ms.[18]

$$bR \xrightarrow{h\nu} K \rightarrow L \rightarrow M_1 \text{ or } M_2 \xrightarrow{h\nu,\ 200ns} bR \quad (2)$$

Hessling et al. have demonstrated that the depletion of the M intermediate occurs upon exposure of the photocycle to an additional blue-flash light resulting in the retinal isomerization from 13-cis to all-trans in picoseconds followed by the reprotonation of the Schiff base returning to its bR state by FT-IR study.[18] Our recent study on the photocurrent from bR has indicated that the photocurrent density is greatly enhanced when the electrochemical cell is exposed to blue light in the presence

* To whom correspondence should be addressed. E-mail: melsayed@gatech.edu.

† These authors contributed equally to this work.

10.1021/jp105468x © 2010 American Chemical Society
Published on Web 08/24/2010

of the plasmonic AgNPs in the bR solutions.[19] The photovoltaic response is due to the change in the proton gradient. We have proposed that the plasmonic field of AgNPs greatly enhances the flux of blue photons which shortcut the photocycle by bypassing the slow paths of the conventional photocycle. This leads to a decrease in the photocycle period and increase in the rate of the proton release, resulting in the enhanced steady-state proton concentration and photocurrent.[19]

The proposed mechanism for the photocurrent enhancement suggest that the blue light effect generated by the plasmonic field of AgNPs greatly perturbs the kinetics of the photocycle.[19] If this is indeed correct, then the rates of the bR ground state recovery and that of the M intermediate decay should both be greatly accelerated by enhancing the blue light absorption rate by the plasmonic field of AgNPs. The kinetics can be studied by using time-resolved spectroscopic technique, and these results can help to quantify the degree of enhanced blue light effect of the acceleration of bR photocurrent by the plasmonic field of AgNPs.

Upon the resonant excitation of the metallic nanoparticles, an intense plasmonic field is generated. The plasmonic field effect on radiative properties have been observed in many systems.[20–22] Previous publications on the plasmonic field effects on bR processes have also been investigated.[23,24] The previous reports showed that the retinal isomerization of bR in the I → J transition can be decelerated and the reprotonation of the Schiff base in the M → N transition can be accelerated in the presence of a plasmonic field upon excitation of gold nanoparticles and gold nanorods, respectively.[23,24]

In the present work, a time-resolved transient absorption technique was employed to study the plasmonic field of AgNPs with different sizes on the kinetics of bR photocycle. Due to the difference of the spectral overlap of their plasmonic resonance extinction and the M intermediate absorption, the plasmonic field enhancement of the blue photon effect will be different. These experiments can be carried out with continuous blue light exposure upon the photoinitiated bR photocycle with short-pulsed 532-nm laser. Consistent with our proposed mechanism for the photocurrent enhancement, the acceleration of the rate of the bR recovery and the M decay can be a result of bypassing the slow part of the photocycle in the presence of AgNPs and external blue photon exposure simultaneously. The dependence of the observed change in rate on the size of AgNPs is found to be consistent with the dependence of the plasmonic field on size and the degree of overlap of the plasmonic extinction spectrum of each nanoparticle with the absorption spectrum of the M intermediate.

2. Experimental Section

Native bR in the PM from *Halobacterium salinarium* was prepared by a standard method described by Oesterhelt and Stoeckenius in 1974.[25] Strain S-9, with a higher PM yield and an absence of carotenoids, was chosen for these experiments. The PM suspension was stored at −10 °C for further use. The bR solutions were light adapted before the measurements.

The synthesis of silver nanoparticles is carried out by the reduction of silver ions (from $AgNO_3$) with sodium citrate or sodium borohydride to synthesize nanoparticles with sizes of 40 and 8 nm, respectively. Samples were freshly prepared by mixing fixed amounts of bR with different amounts of silver nanoparticle suspensions in pH = 7 buffer solution (citrate, 10 mM). Concentrations were controlled such that the buffer solution and bR suspension are 1.1 mM and 8.8 μM, respectively, in each sample. The concentrations of 8-nm and 40-nm AgNPs were adjusted to 75−300 nM and 0.5−2.0 nM, respectively. UV−vis spectra for all samples were acquired using a steady-state spectrometer (HR4000VG-UV-NIR, Ocean Optics) before and after the time-resolved experiments.

SCHEME 1: Experimental Setup of the Pulsed Laser (532 nm) and cw Blue Light (350−500 nm) Photoexcitation of bR

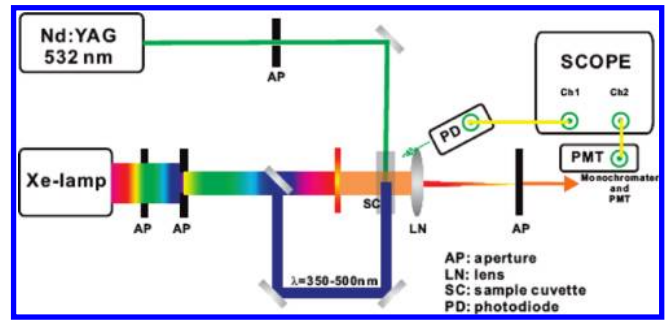

The experimental setup of the short-pulsed laser excitation is drawn in Scheme 1. A frequency-doubled Nd:YAG laser (GCR-2, Spectral Physics) was employed for excitation at 532 nm with a bandwidth of 10 ns, repetition rate of 10 Hz, and a fluence of 5.5 mJ cm^{-2} within 5% energy fluctuation. An optical fiber was employed to introduce the broadband light from a xenon lamp filtered in 350−500 nm for the excitation of silver nanoparticles, with corresponding power 0.12 W cm^{-2}. The excitation laser beam and the continuous wavelength (cw) blue light passed through the sample cell in opposite directions and overlapped in the center of the sample cell. Partial xenon lamp luminosity was employed for continuous probing combined with optical filters and a monochromator (SpectraPro-300i, Acton Research Corporation) to define the detection wavelength at 600 or 450 nm for monitoring the bR and M intermediate, respectively. A photomultiplier tube (R1527, Hamamatsu) was utilized for collecting a photon signal and a 500-MHz transient digitizer (9350A, LeCroy) was used for data acquisition and storage. The temporal profiles of the bR recovery were recorded by probing the photon intensity modulation at 600 nm, and 3000 or 8000 laser shots were averaged depending on the signal-to-noise ratios. The intensity of the M intermediate at 450 nm is relatively weaker than that of bR state, thus the temporal profiles of the M intermediate were averaged in 10 000 laser shot. The temporally resolved absorbance change can be derived by the equation, $\Delta A = \log(S_t/S_o)$, where S_t and S_o represent the dc-coupled voltage in the presence and absence of the excitation laser, respectively.

3. Results

The absorption contour and extinction band of the surface plasmon resonance regions of the AgNPs are adjustable by controlling their size distributions. Figure 1 shows the normalized absorption contours of the bR (purple) and the M intermediate (blue). The 40-nm AgNPs (brown) whose corresponding extinction maximum at 430 nm exhibits greater spectral overlap with the M intermediate absorption band than the 8-nm particles (orange), whose maximum peak is at 397 nm.

The above spectra are obtained by decomposing the observed spectrum into a contribution from pure bR absorption and AgNPs extinction. The extinction of AgNPs is at wavelengths shorter than 600 nm, which eliminates the spectral overlap with the bR absorption and the interference with the monitored temporal profile. Previous results have shown that the M

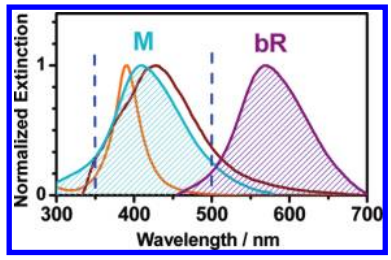

Figure 1. Normalized surface plasmon resonance spectra of 8 nm (orange) and 40 nm (brown) Ag NPs. The absorption contours of M and bR species are represented by blue and purple shadows with corresponding maxima at 412 and 570 nm, respectively. The bR photocycle is photoinitiated by the short-pulsed 532-nm laser and the continuous blue light exposure is between 350−550 nm (shown in blue dash lines). The monitor window of the recovery of bR and the decy of M intermediate are followed at 600 nm and 450 respectively to avoid the spectral overlap with AgNPs and laser scattering.

intermediate absorbs one blue photon to return to the bR ground state without passing through the slow conventional photocycle.[18,26] If this is the reason for our previously reported plasmonic enhancement of the bR photocurrent, then the cooperation of the plasmonic field effect and the blue light effect on the kinetics of bR photocycle should be observed. Furthermore, the degree of perturbation of the different sizes of AgNPs on the kinetics of bR photocycle should be strongly correlated with the overlap between the extinction of the AgNPs and the M absorption band.

The 532-nm pulsed laser and the cw blue light were collimated in opposite directions and overlapped at the center of the sample cell, as shown in Scheme 1. After the short pulsed irradiation from the 532-nm laser for 50 μs, the dominant components of the modulation at 600 nm absorption ($\Delta A_{600}(t)$) are the L decay and the bR recovery.[8] Although the N intermediate exhibits absorption at 600 nm, the transient concentration of the N intermediate has been proven to be low in the photocycle when the pH is controlled at ~7.[27] In addition to the observation of the recovery of bR, the light modulation at 450 nm ($\Delta A_{450}(t)$) reflects the kinetics of the M intermediate.

The recovery of bR upon 532-nm pulsed laser excitation was monitored at 600 nm in the presence and the absence of exposure to the external blue light. Studies were carried out with addition of two sizes of AgNPs (8 and 40 nm). The dependence of the kinetics on the plasmonic field of these two sizes was compared.

Figure 2 represents the temporal profiles of the bR recovery in the presence and absence of blue light by adding AgNPs of 8-nm (A) and 40-nm (B), respectively. Upon excitation of the pure bR suspension, the simultaneous cw blue light exposure resulted in the acceleration of the recovery of the bR state. The addition of AgNPs (either 40 or 8 nm AgNPs) accelerates the bR recovery rate even without introducing the blue light to the systems. However, when both conditions were achieved (the addition of AgNPs and cw blue light), the bR recovery rate was significantly accelerated.

The blue light effect is shown to accelerate the recovery rate of bR. However, it is difficult to monitor the kinetics of the M intermediate at its absorption maximum by time-resolved spectroscopy because of the large overlap between the spectral regions of the 40 nm AgNPs and the M state. As a result, only 8 nm-AgNPs can be used with bR for observing the kinetics of the M intermediate. The monitoring window is set at 450 nm to avoid interference from the extinction of the 8 nm-AgNPs. The main component of the temporal profile at 450 nm is attributed to the M intermediate absorption (See Figure 1). On

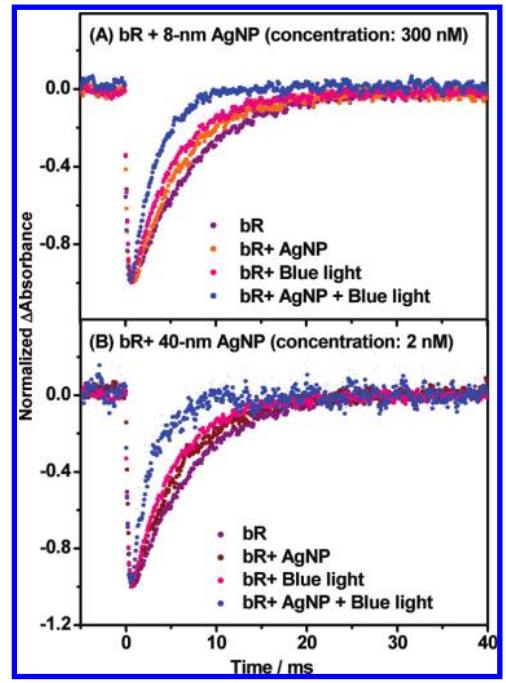

Figure 2. The plasmonic field enhancement of the blue light effect on the bR recovery during its photocycle. Normalized temporal profiles of the modulation at 600 nm upon 532-nm pulsed excitation of the mixtures of bR with (A) 8-nm AgNP and (B) 40-nm AgNP in the presence of cw blue photon (350−500 nm). The addition of AgNPs and exposure to the blue light accelerate the bR recovery. The concentration of buffer solution, bR, 8-nm AgNP, and 40-nm AgNP are 1.1 mM, 8.8 μM, 300 nM, and 2.0 nM, respectively. The power of the cw blue irradiation (in 350−500 nm) is 0.12 W cm^{-2} and the fluence of the 532-nm pulsed laser is 5.5 mJ cm^{-2}.

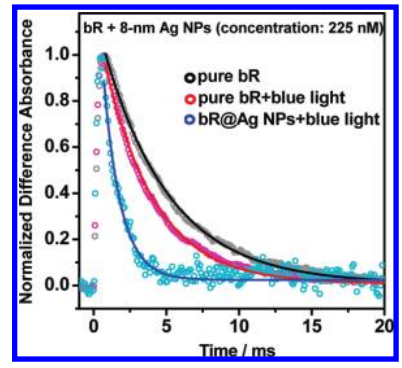

Figure 3. Plasmonic field enhancement of the blue light effect on the decay of M intermediate during its photocycle. The effect on the decay of the M intermediate (black), in presence of blue light (red), and by the plasomincally enhanced blue light effect (blue). Normalized temporal profiles of the modulation at 450 nm upon 532-nm pulsed excitation of the mixtures of bR with 8 nm Ag NPs in the presence of continuous irradiation of blue photon (350−500 nm). The concentration of 8-nm AgNPs is 225 nM. The power of the cw blue light is 0.12 W cm^{-2} and the fluence of the 532-nm pulsed laser is 5.5 mJ cm^{-2}, respectively.

the basis of our proposed mechanism, the decay of the M intermediate can be described by single exponential curve. In Figure 3, the colored circles and their corresponding solid lines represent the observed and fitted data, respectively. The fitted data agree well with the observed temporal profiles. Similar to the results of the bR recovery rate, the decay of the M intermediate was accelerated by the addition of Ag NPs or by exposure to the blue light. A more pronounced acceleration of the M decay was observed by exposure to the blue light in the

presence of AgNPs The accelerated decay of the M intermediate was consistent with the recovery of bR when monitored at 600 nm.

4. Discussion

In order to illustrate the temporal behavior of the bR recovery, the following simplified mechanism is used:

$$\mathrm{bR} \xrightarrow{h\nu(\phi)} \mathrm{L} \xrightarrow{k_1} \mathrm{M} \xrightarrow{k_2} \mathrm{bR}$$

k_2: the rate constant of conventional cycle (no blue light)

$$\xrightarrow{k_3} \mathrm{bR}$$

k_3: the rate constant of bypassed cycle (with blue light) (3)

A detailed mathematical expression of the time dependence of the bR concentration ($\Delta A_{600}(t)$) and the time dependence of the M intermediate concentration ($\Delta A_{450}(t)$) is developed in the Appendix. The constant k_{II} is the apparent rate of the conversion of M to bR. In the absence of cw blue light exposure, only the conventional photocycle should be considered and k_{II} is merely composed of k_2 for the conventional photocycle ($k_{II} = k_2$). Upon the irradiation with the cw blue light, the bypassed photocycle is activated. Thus, k_{II} is composed of both k_2 and k_3, which denotes the apparent rate constant of the conversion of M to bR through the bypassed process ($k_{II} = k_2 + k_3$). The variables k_1 and k_{II} are derived by fitting the observed temporal profiles with two exponential components. The difference of k_{II} in presence and absence of blue light is due to k_3, which represents the rate constant of the bypassed cycle and measures blue light effect.

The comparisons of the observed and fitted data are shown in Figure 4. The minor residual intensities, derived from the difference of the observed and fitted temporal profiles, are also shown in each figure. Due to the strong light scattering from the 40 nm-Ag NPs, the signal-to-noise ratio is relatively smaller than that of the others (Figure 4). However, the observed agreement and the worse residual intensity show that the proposed mechanism agrees well with the observed data.

Both sizes of Ag NPs show the ability to change the kinetics of the bR photocycle. However, the concentration of 8 nm-AgNPs was 100× higher than that of the 40 nm particles (Figure 2). The rate constant of bR recovery in various concentrations of AgNPs are summarized in Figure 5a. Without exposure to blue light, the addition of AgNPs is also able to slightly accelerate the rate of bR recovery. With exposure to the cw blue light, the enhancement is much more significant. Moreover, this effect is more noticeable for AgNPs with large size (40 nm) than that for the small particles (8 nm). According to our proposed mechanism, the difference stands for the rate constant of the bypassed photocycle, denoted by k_3, involving the photoexcitation of the M intermediate followed by the rapid reprotonation and isomerization of retinal converting to its initial bR state (Figure 5b).

Although the concentration of the 40 nm Ag NPs is 100× lower than that of the 8 nm Ag NPs, the larger Ag NPs still show more pronounced enhancement of the blue light effect. The broader absorption band of 40 nm Ag NPs can absorb more of the blue light, thus enhancing the flux of blue photons more than 8 nm particles under the same intensity of illumination.

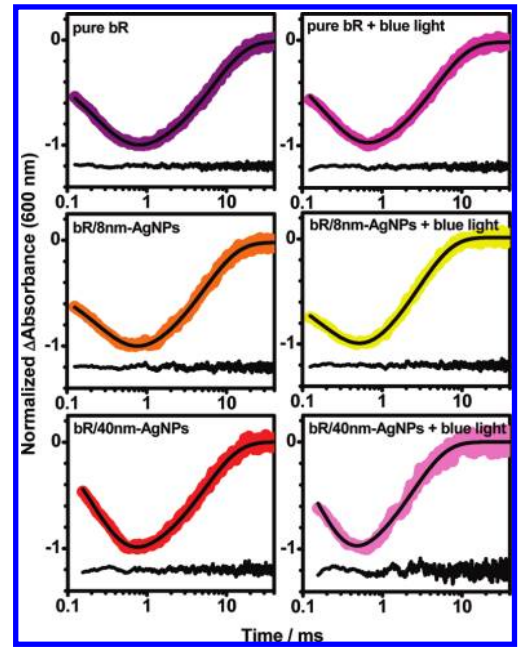

Figure 4. The comparisons of the experimental (color traces) and the fitted data (black lines) of the 600-nm modulation (bR recovery) for pure bR or bR/Ag NPs mixture upon 532-nm pulsed excitation in the absence or in the presence of blue photon. The differences of the observed and the fitted data (residual intensities) are also shown in black at the bottom traces in every part.

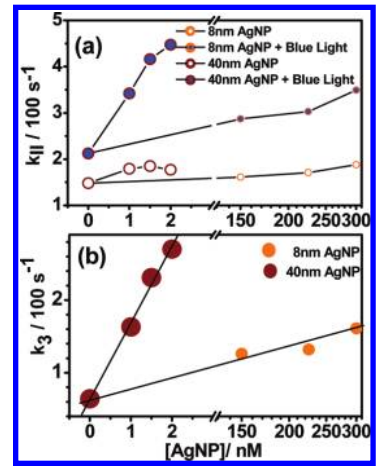

Figure 5. (a) The rate constant k_{II} in the presence and absence of blue light up upon excitation of bR with different concentrations of 8-nm and 40-nm AgNP. (b) The difference of the values of k_{II} in the presence and absence of blue light. The difference can be attributed to k_3, which represents the rate constant of the bypassed cycle, i.e., it represents the sensitivity of the plasmonic field enhancement of the blue light effect to the concentration and size of the nanoparticles used.

In order to get a quantitative experimental measurement of the relative plasmonic enhancement of the blue light effect of the 40 and the 8 nm AgNPs, the ratio of the k_3 value per particle needs to be determined. This can be determined from the ratios of the slopes of the lines in Figure 5b. This ratio is found to be around 400. The value of enhancement factor of each particle depends on a number of factors: (1) the plasmonic field strength, as it determines the enhancement of the M absorption. Su et al. have shown that the field strength is proportional to the size of nanoparticle. Using the radii of the 40 nm and the 8 nm of

AgNPs, the ratio of their sizes is 125.[28,29] (2) The second factor is the transfer rate of the energy between the plasmonic field and the M intermediate, which is proportional to the spectral overlap between the electromagnetic extinction band and the M absorption band. This ratio from the 40- and 8-nm AgNPs is determined to be 3 from Figure 1. Theses two factors alone suggest that the ratio of plasmon enhancement factor of the two nanoparticles used is around 375, which is close to that observed experimentally.

This agreement might suggest that the exact location of each nanoparticle is not critical. This is due to large size of the nanoparticles, even the small one compared to the size of the active site of retinal in the protein. Thus the retinals in the strongest regions of the field of each nanoparticle are the ones that show the observed enhancements.

5. Conclusions

Using time-resolved spectroscopic techniques, we were able to study the plasmonic field enhancement of the observed blue light effect on the bR photocycle. The observed blue light enhancement of the bR recovery and of the M intermediates decay give strong support for the previously proposed mechanism of the blue light photocurrent enhancement.[19] The bypassed photocycle can be activated by exposure to blue light and is greatly enhanced in the presence of AgNPs, whose surface plasmon field is in the blue spectral region (and can thus greatly enhance the flux of blue light). It is found that the 40-nm AgNPs are about 400× more efficient than the 8-nm because of the much larger field strength and better overlap between their extinction band and that of the M intermediate absorption band.

Appendix

Expression of $[L]_t$. On the basis of the report by R. R. Birge et al. (ref 8), the decay rate constant of the L intermediate is slower than that of the generation. Due to the temporal integration window of 10 μs, which is slower than the L generation, the temporal behavior of L can be simplified in a decay component and described as follows,

$$\frac{d[\mathrm{L}]}{dt} = -k_1[\mathrm{L}].$$

An assumption can be made that the initial concentration of L (denoted as $[L]_0$) is proportional to the quantum yield of bR upon 532-nm pulsed excitation.

$[\mathrm{L}]_o = [\mathrm{bR}]_o \times \phi$, ϕ represents the quantum yield of bR bleach

By means of Laplace transform ($\boldsymbol{L}$),

$$\frac{d[\mathrm{L}]}{dt} = -k_1[\mathrm{L}], \therefore \boldsymbol{L}[\mathrm{L}]' = s\boldsymbol{L}[\mathrm{L}] - [\mathrm{L}]_{o=} - k_1\boldsymbol{L}[\mathrm{L}]$$
$$\therefore (s + k_1)\boldsymbol{L}[\mathrm{L}] = [\mathrm{L}]_o = [\mathrm{bR}]_o \times \phi$$
$$\therefore \boldsymbol{L}[\mathrm{L}] = \frac{[\mathrm{bR}]_o \times \phi}{(s + k_1)}$$

As a result, the temporal profile of L can be expressed as follows:

$$[\mathrm{L}]_t = [\mathrm{bR}]_o \times \phi \times e^{-k_1 t}$$

Expression of $[M]_t$.

$$\frac{d[\mathrm{M}]}{dt} = k_1[\mathrm{L}] - (k_2 + k_3)[\mathrm{M}], \text{ set } k_2 + k_3 = k_{\mathrm{II}}$$
$$\therefore \boldsymbol{L}[\mathrm{M}]' = s\boldsymbol{L}[\mathrm{M}] - 0 = k_1\boldsymbol{L}[\mathrm{L}] - k_{\mathrm{II}}\boldsymbol{L}[\mathrm{M}]$$
$$\therefore (s + k_{\mathrm{II}})\boldsymbol{L}[\mathrm{M}] = k_1\boldsymbol{L}[\mathrm{L}] = \frac{k_1 \times [\mathrm{bR}]_o \times \phi}{(s + k_1)}$$
$$\therefore \boldsymbol{L}[\mathrm{M}] = \frac{k_1 \times [\mathrm{bR}]_o \times \phi}{(s + k_1)(s + k_{\mathrm{II}})}$$
$$\therefore [\mathrm{M}]_t = \frac{k_1 \times [\mathrm{bR}]_o \times \phi}{k_1 - k_{\mathrm{II}}} \times (e^{-k_{\mathrm{II}}t} - e^{-k_1 t})$$

Expression of $[bR]_t$ Recovery.

$$\frac{d[\mathrm{bR}]}{dt} = (k_2 + k_3)[\mathrm{M}] = k_{\mathrm{II}}[\mathrm{M}]$$
$$\therefore \boldsymbol{L}[\mathrm{bR}]' = s\boldsymbol{L}[\mathrm{bR}] - 0 = k_{\mathrm{II}}\boldsymbol{L}[\mathrm{M}] = \frac{k_1 \times k_{\mathrm{II}} \times [\mathrm{bR}]_o \times \phi}{(s + k_1)(s + k_{\mathrm{II}})}$$
$$\therefore \boldsymbol{L}[\mathrm{bR}] = \frac{k_1 \times k_{\mathrm{II}} \times [\mathrm{bR}]_o \times \phi}{s(s + k_1)(s + k_{\mathrm{II}})} = \frac{k_1 \times k_{\mathrm{II}} \times [\mathrm{bR}]_o \times \phi}{(k_{\mathrm{II}} - k_1)} \times \left(\frac{1}{s(s + k_1)} - \frac{1}{s(s + k_{\mathrm{II}})}\right)$$
$$\therefore [\mathrm{bR}]_t = \frac{k_1 \times k_{\mathrm{II}} \times [\mathrm{bR}]_o \times \phi}{(k_{\mathrm{II}} - k_1)}\left(\frac{1}{k_1}(1 - e^{-k_1 t}) - \frac{1}{k_{\mathrm{II}}}(1 - e^{-k_{\mathrm{II}}t})\right)$$

Expression of $\Delta A_{600}(t)$. The overall absorbance modulation at 600 nm (ΔA_{600}) should include L decay and bR recovery. Due to the different absorption constants, two weighting parameters (a and b for bR and L, respectively) should be introduced,

$$\Delta A_{600} = -[\mathrm{bR}]_o \times \phi \times (a \times e^{-k_1 t} - b \times e^{-k_{\mathrm{II}}t})$$

An equation is employed in fitting, $\therefore \Delta A_{600} = y = y_0 + c \times e^{-dt} - g \times e^{-ht}$, d and h represent k_1 and k_{II}, respectively.

Expression of $\Delta A_{450}(t)$. The absorbance modulation at 450 nm (ΔA_{450}) is merely composed of the M intermediate and can be expressed as follows:

$$\therefore \Delta A_{450} = a \times (e^{-k_{\mathrm{II}}t} - e^{-k_1 t})$$

When $k_1 \gg k_{\mathrm{II}}$ at later period, ΔA_{450} can be expressed in a single exponential decay as follows:

$$\Delta A_{450} \approx [\mathrm{bR}]_o \times \phi \times e^{-k_{\mathrm{II}}t}$$

Acknowledgment. We would like to thank the U.S. Department of Energy, Office of Basic Energy Grant No. DE-FG02-97-ER 14799. We also thank Mrs. Rachel Near for her carefully revising this manuscript.

References and Notes

(1) Oesterhelt, D.; Stoeckenius, W. *Nature New Biol.* **1971**, *233*, 149.
(2) Pebay-Peyroula, E.; Rummel, G.; Rosenbusch, J. P.; Landau, E. M. *Science* **1997**, *277*, 1676.

(3) Essen, L.-O.; Siegert, R.; Lehmann, W. D.; Oesterhelt, D. *Proc. Natl. Acad. Sci. U. S. A.* **1998**, *95*, 11673.
(4) Luecke, H.; Richter, H.-T.; Lanyi, J. K. *Science* **1998**, *280*, 1934.
(5) Luecke, H.; Schobert, B.; Richter, H.-T.; Cartailler, J.-P.; Lanyi, J. K. *J. Mol. Biol.* **1999**, *291*, 899.
(6) Edman, K.; Nollert, P.; Royant, A.; Belrhali, H.; Pebay-Peyroula, E.; Hajdu, J.; Neutze, R.; Landau, E. M. *Nature* **1999**, *401*, 822.
(7) Rehorek, M.; Heyn, M. P. *Biochemistry* **1979**, *18*, 4977.
(8) Birge, R. R.; Gillespie, N. B.; Izaguirre, E. W.; Kusnetzow, A.; Lawrence, A. F.; Singh, D.; Song, Q. W.; Schmidt, E.; Stuart, J. A.; Seetharaman, S.; Wise, K. J. *J. Phys. Chem. B* **1999**, *103*, 10746.
(9) Lanyi, J. K.; Váró, G. *Isr. J. Chem.* **1995**, *35*, 365.
(10) Váró, G.; Lanyi, J. K. *Biochemistry* **1991**, *30*, 5008.
(11) Váró, G.; Lanyi, J. K. *Biochemistry* **1991**, *30*, 5016.
(12) Váró, G.; Lanyi, J. K. *Biochemistry* **1991**, *30*, 7165.
(13) Subramaniam, S.; Lindahl, M.; Bullough, P.; Faruqi, A. R.; Tittor, J.; Oesterhelt, D.; Brown, L.; Lanyi, J. K.; Henderson, R. *J. Mol. Biol.* **1999**, *287*, 145.
(14) Spassov, V. Z.; Luecke, H.; Gerwert, K.; Bashford, D. *J. Mol. Biol.* **2001**, *312*, 203.
(15) Zimányi, L.; Váró, G.; Chang, M.; Ni, B.; Needleman, R.; Lanyi, J. K. *Biochemistry* **1992**, *31*, 8535.
(16) Gergely, C.; Zimányi, L.; Váró, G. *J. Phys. Chem. B* **1997**, *101*, 9390.
(17) Braiman, M. S.; Bousché, O.; Rothschild, K. J. *Proc. Natl. Acad. Sci. U. S. A.* **1991**, *88*, 2388.
(18) Hessling, B.; Herbst, J.; Rammelsberg, R.; Gerwert, K. *Biophys. J.* **1997**, *73*, 2081.
(19) Yen, C. W.; Chu, L.-K.; El-Sayed, M. A. *J. Am. Chem. Soc.* **2010**, *132*, 7250.
(20) Neretina, S.; Qian, W.; Dreaden, E. C.; El-Sayed, M. A.; Hughes, R. A.; Preston, J. S.; Mascher, P. *Nano Lett.* **2008**, *8*, 2410.
(21) Huang, X.; El-Sayed, I. H.; Qian, W.; El-Sayed, M. A. *J. Am. Chem. Soc.* **2006**, *128*, 2115.
(22) Yen, C. W.; El-Sayed, M. A. *J. Phys. Chem. C* **2009**, *113*, 19585.
(23) Biesso, A.; Qian, W.; El-Sayed, M. A. *J. Am. Chem. Soc.* **2008**, *130*, 3258.
(24) Biesso, A.; Qian, W.; Huang, X. H.; El-Sayed, M. A. *J. Am. Chem. Soc.* **2009**, *31*, 2442.
(25) Oesterhelt, D.; Stoeckenius, W. *Methods Enzymol.* **1974**, *31*, 667.
(26) Ludmann, K.; Ganea, C.; Váró, G. *J. Photochem. Photobiol. B: Biol.* **1999**, *49*, 23.
(27) Ludmann, K.; Gergely, C.; Váró, G. *Biophys. J.* **1998**, *75*, 3110.
(28) Jain, P. K.; El-Sayed, M. A. *Chem. Phys. Lett.* **2010**, *487*, 153.
(29) Su, K. H.; Wei, Q. H.; Zhang, X.; Mock, J. J.; Smith, D. R.; Schultz, S. *Nano Lett.* **2003**, *3*, 1087.

JP105468X